Japanese Journal of Applied Physics
Vol. 44, No. 7B, 2005, pp. 5354–5357

Analysis of Time-Resolved Tunnel Current Signal in Sub-Picosecond Range Observed by Shaken-Pulse-Pair-Excited Scanning Tunneling Miscroscopy

Osamu TAKEUCHI, Masahiro AOYAMA and Hidemi SHIGEKAWA*

Institute of Applied Physics, 21st Century COE, CREST JST, University of Tsukuba, Tsukuba, Ibaraki 305-8573, Japan

(Received January 17, 2005; accepted February 25, 2005; published July 26, 2005)

The data analysis procedure for the time-resolved tunnel current signal obtained by the shaken-pulse-pair method was studied. The fitting function composed of a step function and two double exponential functions that decay from delay time zero towards negative and positive infinities, respectively, reproduced the experimental data. In the analysis, the effects of the interference of the two pulses in a pulse pair, the finite width of impinging pulses, the amplitude of the delay time modulation and the lock-in time constant were considered, for obtaining accurate decay parameters. [DOI: 10.1143/JJAP.44.5354]

KEYWORDS: scanning tunneling microscopy, temporal resolution, femtosecond laser

A new research field of *femtosecond-angstrom technology* is emerging from the combination of two noble measurement techniques, i.e., the pump-probe ultrafast measurement using a femtosecond pulsed laser and the atom-resolving measurement using a scanning tunneling microscope (STM). In this field, ultrafast phenomena that occur in angstrom regions are investigated to assist the fundamental understanding in the basic research of science and the improvement of the future nanotechnology. There have been several approaches proposed thus far to realize such measurement.[1–10] Among them, we adopted the pulse-pair-excited STM (PPX-STM) method as the best candidate to accomplish both femtosecond and angstrom resolutions, and have proposed the shaken-pulse-pair-excited STM (SPPX-STM) setup, which can detect a small time-resolved tunnel current signal with a high precision, avoiding the tip-expansion/shrinking problem caused by the heat brought by laser illumination.[8–10] In the present study, we investigate the analysis procedure of the time-resolved tunnel current signal obtained by SPPX-STM measurement. In this procedure, the accurate decay parameters of the ultrafast transient states are retrieved from experimental data, with eliminating the distortion due to the finite temporal width of laser pulses, the interference of the paired pulses, the shaking amplitude and the time constant of lock-in detection.

In a PPX-STM measurement, the tunnel gap of an STM is illuminated by a sequence of paired laser pulses, typically, with the pulse width t_{pulse} of 10–100 fs, delay time between paired two pulses t_{d} of $\lesssim$500 ps and inter-pulse-pair period t_{rep} of $\sim$10 ns. Since t_{rep} is so short, the current–voltage converter (IVC) of the STM, whose typical cutoff frequency is $\sim$100 kHz, does not resolve each possible current spike in the instantaneous tunnel current $I_{\mathrm{t}}^{*}(t)$ that is caused by the excitation of a sample by each laser pulse pair. Instead, the IVC merely detects the temporally averaged tunnel current signal $I_{\mathrm{t}}(t_{\mathrm{d}}) = \overline{I_{\mathrm{t}}^{*}(t)}$. Even in such cases, when the dependence of $I_{\mathrm{t}}^{*}(t)$ on the illumination intensity has any nonlinearity, $I_{\mathrm{t}}(t_{\mathrm{d}})$ changes when the delay time t_{d} is swept. This is easily understood as follows. When t_{d} is sufficiently large, two independent current pulses are generated by a pulse pair, each of which corresponds to each laser pulse in the pair. On the other hand, when t_{d} is close to zero, only one current pulse is generated, which is as large as that generated by one laser pulse with a twofold intensity. When nonlinearity exists, the total intensity of current pulses is different in these two cases, and it can be observed in the temporally averaged tunnel current $I_{\mathrm{t}}(t_{\mathrm{d}})$. In an intermediate case, the second laser pulse impinges the sample in an excited state by the first pulse. The current spike due to the second laser pulse has a different amplitude from that due to the first laser pulse even when the two laser pulses have exactly the same intensity. The amplitude of the second current pulse is measured in $I_{\mathrm{t}}(t_{\mathrm{d}})$ as a function of t_{d}.

Consequently, the time-resolved tunnel current signal $I_{\mathrm{t}}(t_{\mathrm{d}})$ shows either a peak or a dip at $t_{\mathrm{d}} = 0$ and decays on both negative ($t_{\mathrm{d}} < 0$) and positive ($t_{\mathrm{d}} > 0$) sides. Whether a peak or dip appears is dependent on specific physical systems. We obtain the lifetime of the photoexcited state of the sample from the decay of the $I_{\mathrm{t}}(t_{\mathrm{d}})$ curve. When the two pulses have the same intensity, the curve is symmetric against $t_{\mathrm{d}} = 0$. In comparison with a conventional purely optical pump-probe measurement, the first pulse in a pulse pair is used for pumping the sample, and the tunnel current change due to the second pulse is detected as the probe signal. Since the measurement probes the tunnel current, this method has an angstrom spatial resolution in addition to a femtosecond time resolution based on the pump-probe mechanism.

In practice, how to detect the very small delay-time-dependent component of $I_{\mathrm{t}}(t_{\mathrm{d}})$ with a sufficient accuracy becomes the main problem. One has to detect a 1 fA–1 pA deviation of $\sim$1 nA tunnel current. In the SPPX-STM measurement technique, t_{d} is modulated periodically as $t_{\mathrm{d}} = t_{\mathrm{d}}^{0} + \Delta t_{\mathrm{d}} \sin \omega t$, and $I_{\mathrm{t}}(t_{\mathrm{d}})$ is processed by a lock-in amplifier. As described previously,[8] this method enables the elimination of the broadband noise in a tunnel current signal without introducing thermal expansion and shrinking of the STM tip. The obtained signal corresponds to the differentiated tunnel current by the delay time, $\mathrm{d}I_{\mathrm{t}}/\mathrm{d}t_{\mathrm{d}}$. We can numerically integrate the signal to obtain the $I_{\mathrm{t}}(t_{\mathrm{d}})$ curve.

As described in detail elsewhere,[10] we have recently succeeded in observing a time-resolved tunnel current signal from a low-temperature-grown $GaN_{\alpha}As_{1-\alpha}$ ($\alpha = 0.36\%$) sample. In this study, we consider the data analysis procedure to retrieve the accurate decay parameters of the photoexcited ultrafast states from the obtained results.

The measurement was carried out under the following conditions. The Ti:Sapphire oscillator emitted laser pulses with an average intensity of 300 mW, a central wavelength of 800 nm, a bandwidth of 30 nm, a pulse width of 25 fs, and

*http://dora.bk.tsukuba.ac.jp/

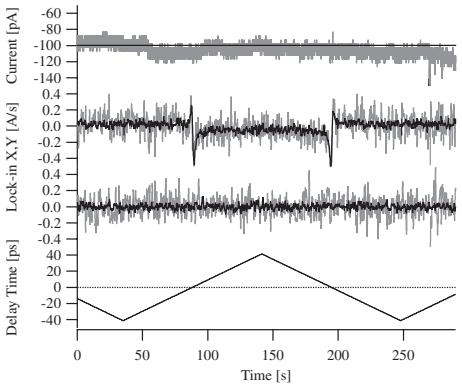

Fig. 1. (a) Tunnel current, (b) in-phase lock-in signal, (c) out-of-phase lock-in signal, and (d) delay time sweep for typical SPPX-STM measurement.

a pulse repetition rate of 80 MHz. The delay line was 150 ps long and the delay line modulation frequency was ~20 Hz. The central value of the modulation was swept by a trianglular wave with a periodicity of ~200 s. The light intensity at the tip-sample gap was ~10 mW and the polarity was *s*-polarized. The effective numerical aperture (NA) of the objective lens was ~20 and the incidence angle of the laser pulses was 40–50° from the surface normal. A weak feedback to the STM *z*-piezo was applied with a cutoff frequency below 0.2 Hz, and the STM set point was adjusted to be 100 pA for a sample bias voltage of −2 V. The first stage of the STM preamplifier had a magnification of $\times 10^9$. The time constant of the lock-in amplifier was 100 ms and the decay slope was −24 dB/oct.

Figure 1 shows a typical experimental result. Raw tunnel current, in-phase and out-of-phase lock-in signals, and delay time are plotted against time for the first 1.5 scans of delay time as gray lines. Although high- and low-frequency noises are included, the peak-to-peak amplitude of the tunnel current fluctuation is less than ±10% of the reference value (100 pA). In an actual measurement, 10–100 sweeps were performed, and the result was averaged in order to reduce the broadband noise. The black lines represent the results obtained as averages of 32 scans. As well known, the noise level is inversely proportional to the square root of the number of scans. Since the thermal drift of the tip-sample position parallel to the sample affects the spatial resolution of the experiment, a highly stable tip position must be achieved to analyze the local structure with a large number of scans. In this experiment, the sample is homogeneous and no spatial variation of the time resolved signal is expected.

Figure 2(a) shows the obtained signal as a function of delay time. The spectrum for the upward scan (solid) and the downward scan (dashed) were separately averaged, each of which represents the data obtained with increasing and decreasing delay time, respectively. Generally, there is a slight shift between the two signals due to the time constant of the lock-in amplifier.

The measured signal is numerically integrated to obtain the delay-time-dependent tunneling current, as shown in Fig. 2(b). Since the integral constant cannot be obtained by the experiment, the absolute value of the tunnel current is undetermined. Here, the value at the left end of the graph is taken to be zero. In this system, the tunnel current increased

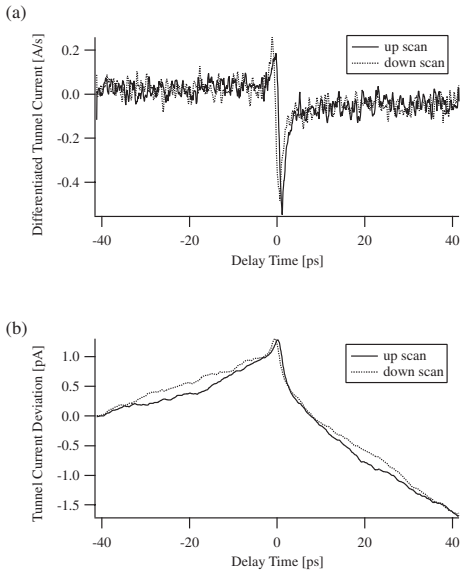

Fig. 2. (a) Raw and (b) integrated signals of SPPX-STM from GaNAs sample.

when the delay time decreased. There are two decay components with a fast (<2 ps) and a slow (~50 ps) decay time. The plot is asymmetric against $t_d = 0$. This is due to the different light intensities of the two pulses (1:2 in this case). The stronger pulse impinged on the sample first in the $t_d < 0$ region.

First, we consider the effect of the interference between the pump and probe pulses. The SPPX-STM method is known to be superior to other methods, because it does not modulate the illumination intensity; thus, the thermal expansion/shrinking problem of the STM tip does not exist. As discussed previously,[8] however, the constant excitation intensity is not preserved when the delay time becomes close to zero. When the delay time is as small as the pulse width, the interference between the two pulses causes the oscillation of the average illumination power. This can have a considerable effect on the tunnel current. How should an interference effect be observed in an experiment?

In an ideal case, the averaged laser power oscillates from zero to twofold the original power by the interference, as shown in Fig. 3(a). This oscillation results in the oscillation in the tunnel current signal shown as the thin line in Fig. 3(b). Such oscillation is induced, for example, by the modulation of tip-sample separation due to the thermal expansion/shrinking of the STM tip and by the modulation of the surface potential of a semiconductor sample due to varying surface photovoltage effect amplitude. In general, the tunnel current dependence on the illumination intensity is highly nonlinear. Thus, the oscillation causes a spike in the low-passed tunnel current signal shown as the thick line.

As the simplest approximation, this tunnel current spike can be considered as a delta function, in comparison with the amplitude of the delay time modulation, Δt_d, in most cases. Then, the tunnel current under the delay time modulation as a function of time can be represented as

$$I_t(t_d^0 + \Delta t_d \sin \omega t) = I_t(t_d^0) + \Delta t_d \frac{dI_t}{dt_d} \sin \omega t + I_t^0 \delta(t_d^0 + \Delta t_d \sin \omega t) \quad (1)$$

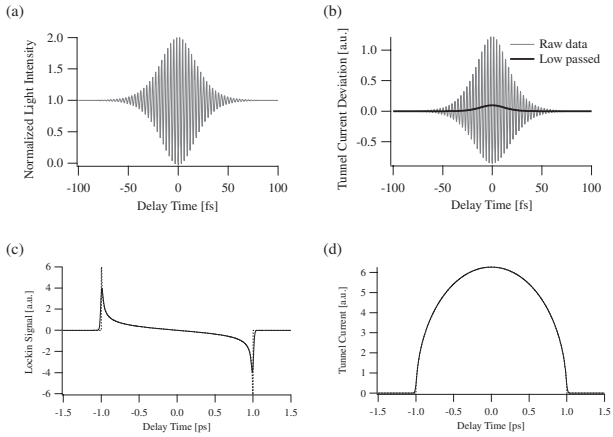

Fig. 3. (a) Illumination intensity oscillating due to intereference effect. (b) Tunnel current response for oscillation. (c) Interference effect in derivative curve for ideally short laser pulse (dotted) and for that of 25 fs width (solid). (d) Integrated signals.

with the angular frequency ω, the center position of the delay time t_d^0 and the current spike intensity I_t^0. Using the relationship $\int \delta(f(x))\mathrm{d}x = \sum_{f(x_n)=0} |1/f'(x_n)|$, the output of the lock-in signal when $-\Delta t_d < t_d^0 < \Delta t_d$ is represented as

$$S(t_d^0) = \frac{\omega}{2\pi}\int I_t(t_d^0 + \Delta t_d \sin\omega t)\cdot\sin\omega t\ \mathrm{d}t = \frac{1}{2}t_d\frac{\mathrm{d}I_t}{\mathrm{d}t_0} + \frac{4\pi}{\Delta t_d}I_t^0\frac{1}{\sqrt{(\Delta t_d/t_d^0)^2-1}}. \quad (2)$$

The calculated value obtained for $\mathrm{d}I_t/\mathrm{d}t_d = 0$ and $\Delta t_d = 1$ ps is shown as a dotted line in Fig. 3(c). In this equation, the signal diverges when $t_d^0 \to \Delta t_d$, which does not happen, however, for a finite pulse width. The result for the pulse width of 25 fs is shown as a solid line. The integration of these curves results in half ellipses with the lateral width of $2\Delta t_d$, as shown in Fig. 3(d).

As determined from the second term of eq. (2), the interference effect on the lock-in signal is proportional to I_t^0 and Δt_d^{-1}. In addition, when the change in I_t^0 is due to the thermal expansion of the STM tip, the amplitude of the signal decreases when $\omega\Delta t_d$ increases. Consequently, the interference signal can be effectively decreased by increasing Δt_d and ω. Actually, interferrence effect was not notable in the present experimental result.

Now we consider the fitting procedure for the experimental data with simple mathematical models. As shown later, for this particular experimental data, two double exponential functions that decay from $t_d = 0$ to negative and positive infinities with a step function at $t_d = 0$ successfully fit the tunnel current response on the delay time, $I_t(t_d)$. Figure 4 shows the fitting function (black line) and its components (gray lines). Two double exponential functions on both positive and negative sides have the same lifetimes, although their amplitudes differ. The magnitude of the step function corresponds to the difference in amplitude between two double exponential functions; thus, the fitting function is continuously connected at $t_d = 0$. This difference in base line indicates the existence of physical process(es) with larger time scale(s). Consequently, there are five parameters to be fit: two lifetimes and two amplitudes for the double

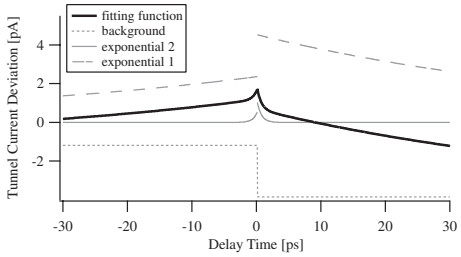

Fig. 4. Fitting function for time-resolved tunnel current spectrum (black) and its components (gray).

exponential function on the positive side, and the relative magnitude between the positive and negative sides. Here, one must note that the absolute base-line position is an arbitrary parameter that cannot be determined by the experiment.

For accurate fitting, one should not directly compare the fitting function mentioned above and an integrated experimental data, because the latter is strongly affected by measurement parameters, such as the laser pulse width, amplitude of the delay time modulation, and lock-in time constant. We must consider these parameters as follows.

The effect of a finite pulse width can be easily considered by convoluting the pulse shape onto the original fitting function. The shape of an ultrashort laser pulse is known to be well approximated by a hyperbolic secant function. Thus, the fitting function is deformed as

$$I_t'(t_d) = A\int I_t(t)\,\mathrm{sech}^2(t - t_d)\mathrm{d}t, \quad (3)$$

with A as the normalizing factor. Typically, the pulse width is chosen to be sufficiently small compared to the decay constants of the physical system. In such cases, this effect is negligible. Otherwise, the analysis suffers from impossibility of distinguishing the interference effect from the ultrafast decay processes. Under the present experimental condition, this effect was negligible.

On the other hand, the delay time modulation and the lock-in detection generally affect the result. The larger the modulation amplitude is, the larger the detected signal we can obtain. In addition, the larger the lock-in time constant is, the less noise the data contains. Thus, a large modulation amplitude with a large lock-in time constant is favorable for maximizing the signal-to-noise ratio. However, such a condition deforms the obtained data considerably. Thus, one must optimize the parameters.

In our experiment, the delay time was controlled by the composition of a triangular wave of ± 40 ps amplitude at 5 mHz and a sinusoid modulation of ± 0.7 ps amplitude at $\sim$20 Hz. The tunnel current expected for this input can be obtained by simply assigning this modulated triangular wave into eq. (3). In the actual measurement, the low-frequency component of the tunnel current signal is compensated by the weak z-feedback of the STM. When the cutoff frequency of the feedback system is chosen properly, however, the influence on the detection of the modulated component is negligible.

In the lock-in amplifier, the tunnel current signal is multiplied by the sinusoid wave at the modulation frequency

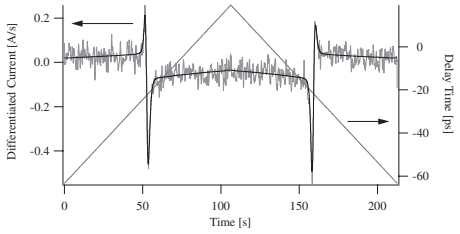

Fig. 5. Experimental (gray) and fitting (black) curves for time-resolved differentiated tunnel current. The delay time sweep is plotted on the right axis.

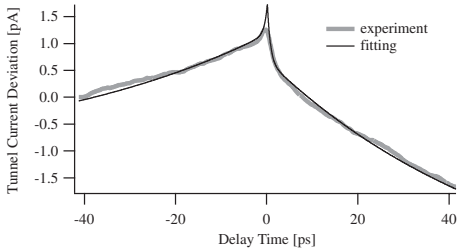

Fig. 6. Integrated spectra from experimental data (gray) and best fit (black).

and then processed by low-pass filter. The low-pass filter is characterized by its time constant T and the decay slope in the high-frequency region. For example, the first-order filter has a slope of $-6\,\mathrm{dB/oct}$, and the second-, third- and fourth-order filters have -12, -18, and $-24\,\mathrm{dB/oct}$ slopes, respectively. The transmission function of the nth filter is represented as $T_n(s) = 1/(1+sT)^n$ and its impulse response is

$$I_{\mathrm{LP}}(t) = Ct^{n-1}\exp(-t/T), \tag{4}$$

with the normalizing factor C. The output of the lock-in amplifier can be numerically simulated by the same procedure, i.e., convoluting the impulse response to the signal after multiplying the sine wave.[11] The calculated result for the best fit is shown by the black line in Fig. 5, with the experimentally obtained averaged signal (gray line) and the delay time. It can be seen that the experimental result is reproduced well, including the asymmetry between the upward scan and the downward scan, which is due to the lock-in time constant.

The fitting is carried out by adjusting the fitting parameters to have the best fit between the experimental data and the finally obtained numerical model. For the present example, the parameters listed in Table I give the best fit. Here, the parameters for the slow decay component have a relatively poor accuracy. This is because the amplitude of the delay time sweep was small. The other parameters, including that of the fast decay component whose decay time is comparable to the amplitude of the delay time modulation, can be accurately obtained. Figure 6 shows the $I_t(t_d)$ curve of the best fit and the integrated experimental data, which was obtained by averaging the data for the upward and downward scans. The disagreement between the two curves indicates the necessity of a careful fitting procedure as discussed above.

Before summarizing the result, we must mention the validity of the model function used in this study for fitting.

Table I. Fitting parameters obtained from SPPX-STM data for GaNAs.

Amplitude of the fast decay component	$0.55 \pm 0.014\,\mathrm{pA}$
Lifetime of the fast decay component	$0.653 \pm 0.025\,\mathrm{ps}$
Amplitude of the slow decay component	$2.36 \pm 0.15\,\mathrm{pA}$
Lifetime of the slow decay component	$55.1 \pm 5.0\,\mathrm{ps}$
Shift of the base line at $t_d = 0$	$2.66 \pm 0.15\,\mathrm{pA}$

Although we observed that the double exponential function reproduced our experimental data considerably well, the detailed analysis that considers the nonlinear dynamics in the sample predicts that the signal does not generally have exponential shapes.[12] Experiments with a higher precision and a wider sweep of delay time must be carried out to discuss the deviation of data from the exponential decay and physical origin of the ultrafast response.

As a summary, the data analysis procedure for the time-resolved tunnel current signal from a shaken-pulse-pair-excited STM measurement was examined. The effects of the interference of the two pulses in a pulse pair, the finite pulse width, the amplitude of the delay time modulation and the time constant of the lock-in detection were considered for obtaining the accurate parameters of the ultrafast transient state of a nanoscale measurement target.

Acknowledgment

This work was supported in part by a Grant-in Aid for Scientific Research from the Ministry of Education, Culture, Sports, Science and Technology, Japan.

1) S. Weiss, D. Botkin, D. F. Ogletree, M. Salmeron and D. S. Chemla: Phys. Status Solidi B **188** (1995) 343.
2) M. R. Freeman, A. Y. Elezzabi, G. M. Steeves and G. Nunes, Jr.: Surf. Sci. **386** (1997) 290.
3) N. N. Khusnatdinov, T. J. Nagle and G. Nunes, Jr.: Appl. Phys. Lett. **77** (2000) 4434.
4) R. J. Hamers and D. G. Cahill: J. Vac. Sci. & Technol. B **9** (1991) 514.
5) M. J. Feldstein, P. Vohringer, W. Wang and N. F. Scherer: J. Phys. Chem. **100** (1996) 4739.
6) V. Gerstner, A. Knoll, W. Pteiffer, A. Thon and G. Gerber: J. Appl. Phys. **88** (2000) 4851.
7) R. H. M. Groeneveld and H. van Kempen: Appl. Phys. Lett. **69** (1996) 2294.
8) O. Takeuchi, R. Morita, M. Yamashita and H. Shigekawa: Jpn. J. Appl. Phys. **41** (2002) 4994.
9) *Mono-Cycle Photonics and Optical Scanning Tunneling Microscopy Route to Femtosecond Angstrom Technology*, eds. M. Yamashita, H. Shigekawa and R. Morita (Springer, Heidelberg, 2005) Springer Series in Optical Sciences, Vol. 99.
10) O. Takeuchi, M. Aoyama, R. Oshima, Y. Okada, H. Oigawa, N. Sano, H. Shigekawa, R. Morita and M. Yamashita: Appl. Phys. Lett. **85** (2004) 3268.
11) By simply following the described procedure, spikes might appear in the calculated signal at the turning points of delay time sweeps. The polarity and height of the peaks depend on the relative phase between the delay time modulation and the sweep. By averaging the number of sweeps with random relative phases, these peaks are smoothed out.
12) O. Takeuchi, M. Aoyama and H. Shigekawa: unpublished.